Masters Program in Geospatial Technologies

Development of a methodology to fill gaps in MODIS LST data for Antarctica

Mohammad Hussein Alasawedah

Dissertation submitted in partial fulfilment of the requirements for the Degree of *Master of Science in Geospatial Technologies*

NOVA IMS Information Management School

Universitat Jaume·I

Westfälische Wilhelms-Universität Münster

Development of a methodology to fill gaps in MODIS LST data for Antarctica

---

Dissertation supervised by

Prof. Dr. Hanna Meyer

University of Münster (WWU)

Münster, Germany

Maite Lezama Valdes

University of Münster (WWU)

Münster, Germany

Prof. Dr. Ignacio Guerrero

Universitat Jaume I Castellón

Castellón, Spain

February 2021

Declaration of Originality

I declare that the work described in this document is my own and not from someone else. All the assistance I have received from other people is duly acknowledged and all the sources (published or not published) are referenced. This work has not been previously evaluated or submitted for any academic degree.

Signature:

Name: Mohammad Hussein Alasawedah

Place: Münster, Germany

Date: 22 February 2021

Acknowledgments

First, thanks to God who gave me the strength and ability to complete this work in the best possible way. Also, I would like to thank Erasmus Mundus scholarship for providing the financial support and give me this wonderful opportunity.

A big thanks to my supervisor Prof. Dr. Hanna Meyer, for giving me this opportunity to work within her research group and for her feedback and support through the thesis journey. A great amount of gratitude goes to co-supervisor Maite Lezama, for her support from the beginning to the end of the thesis; she gave me valuable pieces of advice to carry out this research in the best way. Also, I would like to thank my other co-supervisor Prof. Dr. Ignacio Guerrero, for his support and encouragement.

Special acknowledgment for my parents, my family, and my friends who they were always behind any success in my life.

Abstract

Land Surface Temperature (LST) is an essential parameter for analyzing many environmental questions. Lack of high spatio-temporal resolution of LST data in Antarctica limits the understanding of climatological, ecological processes. The MODIS LST product is a promising source that provides daily LST data at 1 km spatial resolution, but MODIS LST data have gaps due to cloud cover. This research developed a method to fill those gaps with user-defined options to balance processing time and accuracy of MODIS LST data. The presented method combined temporal and spatial interpolation, using the nearest MODIS Aqua/Terra scene for temporal interpolation, Generalized Additive Model (GAM) using 3-dimensional spatial trend surface, elevation, and aspect as covariates. The moving window size controls the number of filled pixels and the prediction accuracy in the temporal interpolation. A large moving window filled more pixels with less accuracy but improved the overall accuracy of the method. The developed method's performance validated and compared to Local Weighted Regression (LWR) using 14 images and Thin Plate Spline (TPS) interpolation by filling different sizes of artificial gaps 3%, 10%, and 25% of valid pixels. The developed method performed better with a low percentage of cloud cover by RMSE ranged between 0.72 to 1.70 but tended to have a higher RMSE with a high percentage of cloud cover.

Acronyms

CNNs	Convolutional Neural Networks
EAIS	East Antarctic Ice Sheet
ELM	Extreme learning machine
ETM+	Enhanced Thematic Mapper Plus
GAM	Generalized Additive Models
LST	Land Surface Temperature
LWR	Local Weighted Regression
MODIS	Moderate Resolution Imaging Spectroradiometer
NASA	National Aeronautics and Space Administration
OLS	Ordinary Least Squares
RAMP	Radarsat Antarctic Mapping Project
RMSE	Root Mean Square Error
TPI	Topographic Position Index
TPS	Thin Plate Spline
TRI	Terrain Ruggedness Index
WAIS	Western Antarctic Ice Sheet

Table of Contents

List of Tables

Table of Figures

1 Introduction

Climate change and ecology research required critical information about land surface temperature (LST), making LST an essential input variable for different related research areas of climate change, ecology, and hydrology [1]. LST is used to drive related bioclimate variables for different ecological models [2]. Therefore, the availability of high spatio-temporal resolution of the temperature dataset is critical in preserving different processes of climatological, hydrological, and ecological [3]. Land surface temperature dataset provided from metrological stations by applied geostatistics interpolation [4,5], but this traditional method is not working correctly when metrological stations are distributed poorly or have limited stations [1,6]. Moreover, it is tough to proceed with geostatistics interpolation methods using metrological stations record in a complex terrain area [7].

Satellite-derived information was an important method to build an accurate and complete land surface temperature (LST) dataset [8,9], Which help to minimize and overcome the obstacles of using metrological stations [1]. Satellite data provide a high spatio-temporal dataset used for different purposes of monitoring and solving environmental problems at local, regional, and global scales [10]. One of the well-known LST sources was produced by Moderate Resolution Imaging Spectroradiometer (MODIS) sensors onboard on Aqua and Terra spacecraft from NASA. The combination of two sensors provides a high temporal resolution of LST data by cover the earth four times every 24 hours, two observations by Aqua and two by Terra, with 1 km spatial resolution across the earth.

However, there is still missing information in MODIS LST data over the world due to cloud contamination. Cloud contamination is one of the serious problems of all remotely sensed data [1,11]. The clouds generate different sizes of gaps in the MODIS LST dataset [12]. Analysis of MODIS LST data showed that a high percentage of missing pixels occurred during the winter [1,2] because of clouds' frequent presence. Most of the outlier present in the negative range because of the cold surface of undetected thin clouds [2], making it very difficult to detect the outliers in the study area when the temperature remains negative [1].

Reconstruct the LST dataset is essential to have a complete LST dataset to use in the different research areas (climate change, ecology, agriculture, etc.). Different approaches have been used to reconstruct LST images, ranging from temporal interpolation, spatial interpolation, spatio-temporal interpolation, and machine learning techniques. Use auxiliary data improved the results of the reconstruction method, most of the studies have used elevation as a predictor for temperature [1,7], adding the emissivity bands as a covariate would improve the results by

increasing the contrast between land cover types, especially over the urban area and large water body [1].

The previous reconstruction methods of MODIS LST data have computational difficulties like many geostatistics parameters or long-time series of images in temporal interpolation, making them very difficult to apply in a daily research routine. This research focuses on developing a methodology of filling gaps in MODIS LST data to use in the daily routine of research without spending too much time balancing computing work and prediction accuracy. By filling the gaps using the nearest scene in time, fill the remaining gaps in space using Generalized Additive Models (GAM) with 2D/3D spatial trend surface to consider the spatial autocorrelation.

1.2 Aim and research questions

This study aims to develop a methodology to fill gaps in MODIS LST data in Antarctica to support climatological, hydrological, or ecological processes. Based on GAM with 3D spatial trend coupled with reconstruction in time. To achieve the aim, the following research questions structured for each part:

Temporal Interpolation

- How could the moving window provide satisfying results in terms of continuity and accuracy?

- What is the best scale of moving window that could use for the study area?

Spatial Interpolation

- What are the most important variables to predict Land Surface Temperature (LST) for the study area?

- What is the best smoothing spatial trend surface that could use?

Spatio-temporal Interpolation

- How accurately could the gaps in LST data be filled?

2 literature review

There are several interpolation methods have been used to fill the gaps in satellite data. These interpolation methods were categorized into three main groups: temporal gap filling using a time series of images, gap-filling in space based on spatial information, and spatio-temporal gap-filling methods. The following subsections will give a background about the filling gaps approach categories and the state-of-art of using machine learning techniques to fill the gap.

2.1 Temporal gap-filling methods

Temporal interpolation used to fill the gaps in satellite images by using a time series of satellite data; making it relies on the fact that the time series arranged depending on their occurrence in time [13], which is rare to find missing values for the same pixel for a long sequence of images in the time series [14]. Linear interpolation is the most straightforward approach used to fill the gaps in time using the closest dates to the target scene [15]. This approach could be more complicated when included more details like the number of nearest neighbors, pixel's weight, and any side of the gap could be included in the filling process [15,1]. The nearest five valid neighbors were used to fill the gaps using Local Weighted Regression [1], while the weighted average of the previous and following seven values of the same pixel were used to fill the gap by giving more considerable influence to the closer distance-time [2].

Another temporal method used to fill the gaps by estimating the missing values from another source for the same type of data, gaps of MODIS LST data reconstructed by taking advantage of the temporal proximity between Aqua and Terra (approximately 3h) [16,17], but this method needs knowledge about fluctuations of temperature in each day [1]. Linear interpolation between Aqua/Terra observations on the same day was used to analyze the relationship between them over different land covers and seasons and then use it to fill the missing pixels [16]. Another method was adding the difference between the seasonal mean LST values of Aqua and Terra to the valid pixels of Terra to remove the fluctuation in LST values, then used Terra to reconstruct Aqua LST data [17]. In another context of filling missing pixels using different sources, SAR images acquired by sentinel-1 were used to fill the gap in optical images obtained from sentinel-2 [18], but this is not an option for thermal information.

A more complex approach was used to fill the gaps in MODIS LST data like harmonic analysis [19] or Temporal Fourier analysis [15] by capturing the

seasonality in the time series data. Also, a novel method relies on the assumption that each missing pixel has similar pixels changed their values in the same way over time, those pixels were selected by similarity function, then use transfer function for each missing pixel to fill the gaps [20].

The main disadvantages of temporal interpolation methods are the impossibility/difficulty of applying them in a cloudy area or during the winter season due to cloud occurrence frequency [15]. That means a high possibility of missing values of the same pixels for a long time, and these methods fill the gaps partially and do not provide a complete gap-free dataset [1,2].

2.2 Gap-filling in space methods

These methods use the information around the missing pixels to interpolate them. Traditional spatial interpolation methods rely on the assumption that neighboring pixels are spatially correlated [20]. However, this assumption could be incorrect in the case of temperature interpolation over a rough/complex terrain area due to the high correlation between elevation and LST values [21], and the traditional spatial interpolation methods (e.g., kriging interpolation, TPS) are unsuitable for interpolating over a significant gap in the image [22] and provide poor results when the data points distributed poorly in the study area [2]. Therefore, using auxiliary data is very important to improve spatial interpolation methods; elevation is the most critical variable used to predict LST [1,2,7].

Non-spatial models (e.g., linear regression and GAM) have been used to fill the gaps in space. Linear regression between valid LST values and associated elevation in a split window centered above the missing pixel used to fill the LST data gap in case of 10% of pixels in that window is valid [22]. However, that would violate the assumption of independence between the observations when using the regression models, and the resulting residuals will also show spatial dependence [23]. Adding the spatial component to the model overcomes this problem by smoothing the interaction between spatial location of observations based on the cell center's coordinates using spline smoothing [24]. Alternatively, spatial regression models (spatial lag and spatial error models) [25] were used to recognize the spatial component in the non-spatial models.

In a different context, a hybrid approach between the regression model and the geostatistical approach was used to fill MODIS EVI data [10]. Generalized Additive Models used to fit the data, then simple kriging applied on the resulted residuals of GAM, and then the kriging residuals added to the predicted values of GAM.

2.3 Spatio-temporal gap-filling methods

Using one of the previous methods individually has disadvantages and limitations, as mentioned above, therefore integrated both methods would improve the results. This approach is useful when the percentage of valid pixels is insufficient to apply spatial interpolation, and the temporal interpolation is not enough to fill all the gaps [1,2].

Spatio-temporal models used a multi-step modeling approach, which means fill the gaps using a sequence of spatial/temporal steps [a]. Metz et al. [2] proposed a novel spatio-temporal approach, used weighted temporal averaging to fill the gaps partially, then use statistical modeling (multiple regression) and spatial interpolation (spline interpolation) to fill the remaining gaps in the MODIS LST data. In 2017, Metz et al. [1] upgraded and improved the method by replacing the weighted temporal averaging by Local Weighted Regression (LWR) because of its ability to capture the short-term fluctuations of LST. Thin Plate Spline (TPS) interpolation with covariates (elevation and emissivity band) to fill the remaining gaps in the image instead of B-spline interpolation because TPS is an exact interpolation preserve on the original LST values of valid pixels after smoothing.

Another approach was using the spatiotemporal gradient method TO reconstruct 8-day MODIS LST data by calculating the difference between the average of all valid pixels and each valid pixel in LST data over time, then fill any missing pixel in the MODIS LST image by adding the average of the gradient for that pixel to the average value of all valid pixels in the same image [14].

2.4 Machine learning techniques

Lately, taking advantage of the deep learning technique's rapid growth as a non-linear expression, it has been used to capture the relationship between cloudy and cloud-free pixels over a time series and use it to fill the gaps [26]. Convolutional Neural Networks (CNNs) used to solve three problems of missing information (deadlines in Aqua MODIS, thick cloud cover, and Landsat ETM+ scan line corrector-off problems) in satellite imagery by using temporal, spatial, and spectral information as input to the Convolutional Neural Networks [27].

Also, Convolutional Neural Network (CNN) was used to fill the gaps of optical image (Sentinal-2) using multi-source data obtained from Sentinal-1 (SAR data) and Sentinal-2 (optimal images) by applying the autoencoder technique [18].

CNN's performance was poor when filling Landsat TM images' gaps due to thick cloud occurrence, resulting in blurry and distorted spectral values [27].

One of the disadvantages of using deep learning techniques to fill the gap is the slow gradient descent-based learning algorithms and the massive amount of data need to fill, which makes this technique highly computing and very slow [26]. Therefore, a novel approach was presented to increase the learning speed and improve the general performance of filling the gap by capturing the continuity of the time space-spectrum of a series of remote sensing images called the Extreme learning machine (ELM) technique [26]. In general, ML techniques to fill the gaps still under development and have many limitations that need to investigate and improve, like the learning speed and overfitting. Therefore, they are still not used to fill the gaps in satellite data in the research daily routine.

3 Methodology

This study suggests a combination method between temporal and spatial interpolation to fill the MODIS LST data gaps due to clouds. The overall methodology is divided into two sections; the first one focuses on filling the gap temporally by using the nearest Terra/Aqua scene on the same day, while the second one focuses on filling the remaining gap in space using the GAM model with the spatial trend surface. The following subsections will describe the study area, processing the data, temporal, and space-filling. Figure 1 illustrates the workflow of the reconstruction method.

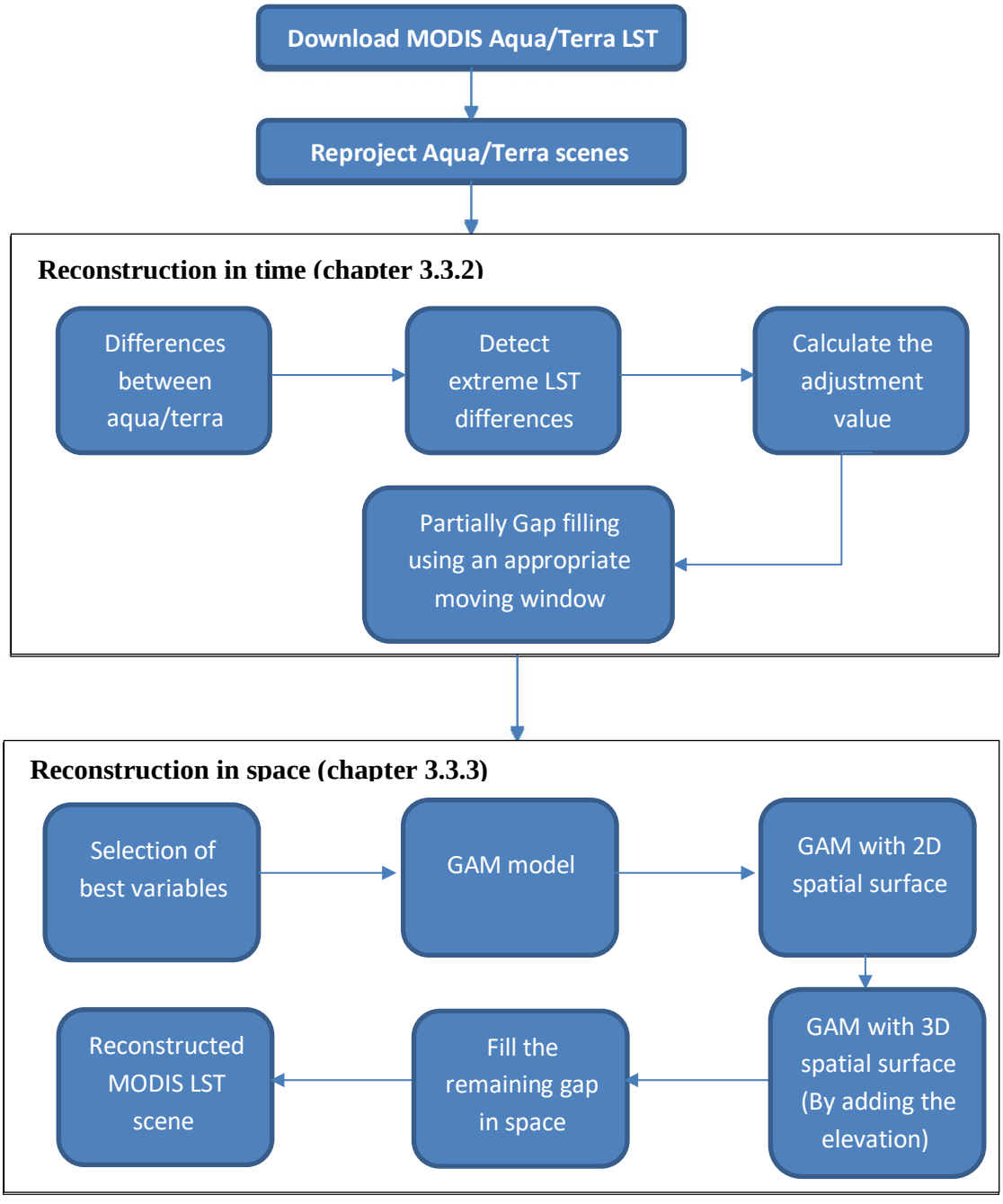

Figure 1. The workflow of the reconstruction method.

3.1 Study area

The research area is the southernmost continent of the earth, located at the south pole called Antarctica. Antarctica is divided into three main regions (Figure 2), namely East Antarctic Ice Sheet (EAIS), Western Antarctic Ice Sheet (WAIS), and Antarctica Peninsula by the total area of approximately 14,200,000 km2. Each region influences differently by climate change [28]. Antarctica is the coldest, driest, and highest continent on the earth by an average elevation of about 2500 m.

Antarctica has more attention to climate change due to the increasing sea level because of ice melting, especially in the west Antarctic [28-30]. LST is an essential variable in monitoring climate warming in Antarctica by capturing the land surface temperature patterns across the continent [31]. Many research stations in Antarctica are doing scientific research in a different area (e.g., climate, hydrology, and ecology). Therefore, the high spatial-temporal resolution of the LST dataset is required for those research areas.

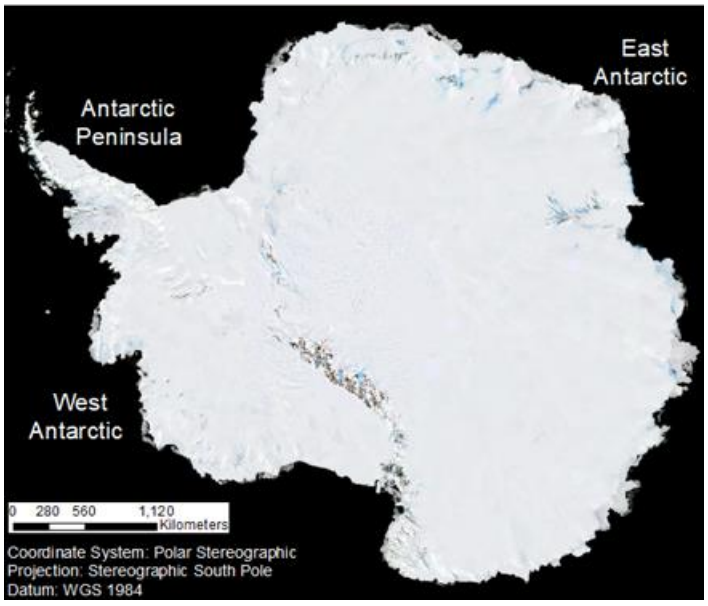

Figure 2. Landsat image mosaic of Antarctica shows the main regions of Antarctica [28,32].

3.2 Data and preprocessing

3.2.1 MODIS data

This study used MODIS LST products MOD11A1/MYD11A1 collection 6, downloaded randomly by MODIS package in R software from LPDAAC/ LAADS servers [33,34]. Day and night Terra /Aqua scenes were downloaded from different seasons in 2016 (15 Jan., 30 Mar, 15 Sep, and 31 Oct), in a total of 8 scenes for each sensor onboard on Aqua and Terra to use in this research. Emissivity 1-Day band delivered alongside daily LST data has the same percentage of missing pixels, which prevents it from being used as a covariate to fill the gaps in daily MODIS LST data. However, the emissivity value does not change in a short time (8 days) because the land cover remains the same. Therefore, the Emissivity 8-Day band delivered with LST products MOD11A2/MYD11A2 has been used as a covariate variable instead of the 1-Day emissivity band 8-Day band is almost free of gaps, and each pixel value represents the average of all pixels within those eight days. R software used to fill the small remaining percentage of missing pixels in the 8-day emissivity band using linear temporal interpolation with other 8-day products in the same month. MODIS data has been projected to Antarctica polar stereographic projected coordinate system, followed by cropping the study area, then convert the unit of LST from Kelvin to Celsius based on MODIS LST product users' guide [35].

3.2.2 Auxiliary Data

Digital Elevation Model (DEM) version 2 created by Radarsat Antarctic Mapping Project (RAMP) has been used [36]. DEM matched the origin and the spatial extent of LST scenes using R software's bilinear resampling method. Antarctica's terrain characteristics extracted from DEM using R software, described by the following variables slope, roughness, aspect, Terrain Ruggedness Index (TRI), and Topographic Position Index (TPI). Solar incidence angle is the angle between the sun's rays and the normal on a surface [37], equation 1 developed by Kreith et al. [38] has been implemented into R function to calculate solar incidence angle for different MODIS scenes :

$$\begin{aligned}\cos(\theta) = {} & \sin(L)\sin(\delta)\cos(\beta) - \cos(L)\sin(\delta)\sin(\beta)\cos(Z) \\ & + \cos(L)\cos(\delta)\cos(h)\cos(\beta) \\ & + \sin(L)\cos(\delta)\cos(h)\sin(\beta)\cos(Z) \\ & + \cos(\delta)\sin(h)\sin(\beta)\sin(Z)\end{aligned} \qquad 1$$

Which θ is the solar incidence angle, L is the latitude location of the surface, β is the surface tilt angle from the horizontal, Z is the surface azimuth angle, h is the Hour angle, and δ is the declination angle. Hour angle (h) is the sun's angular displacement to east or west of the local meridian due to the earth's rotation on its axis, and it is negative in the morning while it is positive in the afternoon [38]. Declination angle (δ) is the angle between the earth-sun line and the earth's equatorial plane [39], each day of the year has its declination angle.

3.3 Methods

3.3.1 Exploratory data analysis

The first step was exploring the data using the descriptive analysis to explore the data and find out the relationship between predictors using correlation matrix, then reduce the dimensionality of the data set by deleting the highly correlated variables. Then, check the percentage of missing pixels for the 16 scenes of MODIS LST to find out later if there is any relation between the percentage of missing pixels and the method's performance.

3.3.2 Reconstruction in time

Aqua day overpass observed on 31 October 2016 filled partially using the nearest Terra overpass on the same day (Figure 3). Filling in time includes three main steps: filter unreliable LST values, choose the moving window's size, and fill gaps using adjustment value.

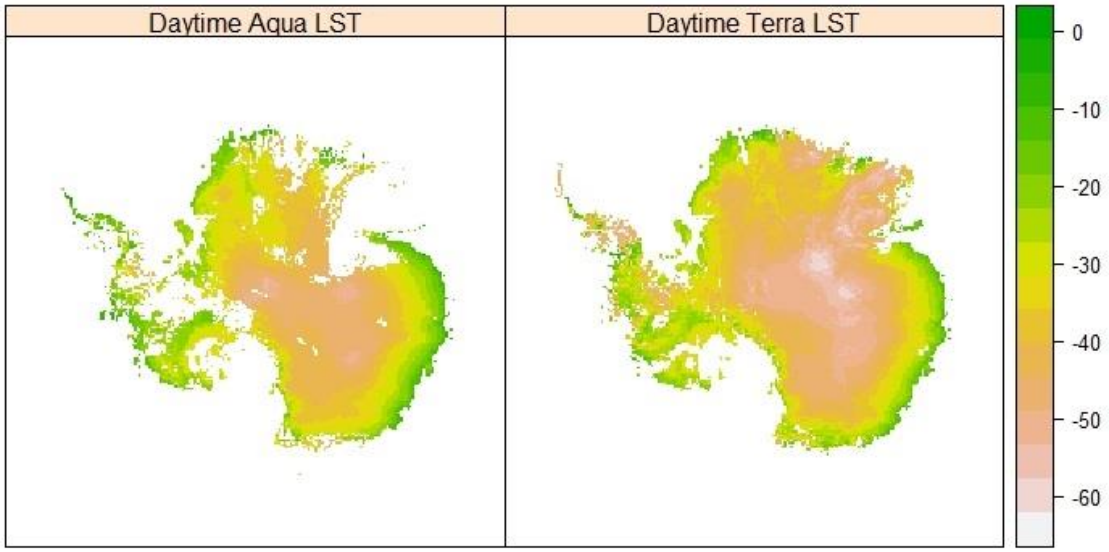

Figure 3. Daytime Aqua and Terra LST scenes (31 October 2016).

3.3.2.1 Filter unreliable values of LST

Aqua and Terra overpasses are very close by approximately 3 hours between each other. However, the undetected thin cloud by the MODIS cloud mask algorithm [40] causes extreme low/high LST values in Aqua/Terra overpasses, leading to significant LST values change. Therefore, big differences between the Aqua/Terra scenes indicate an outlier in one of the two scenes. Therefore, a quantile outlier detector based on the LST difference between Aqua and Terra was used to detect outliers by setting a threshold of LST differences by applied equations 2-3. The detected pixels of significant change were excluded from the adjustment value calculation without deleting them because it is unknown which pixel has very high/very low value (Terra or Aqua).

$$\text{Low threshold} = 1^{st}\ \text{quartile} - (3^{rd}\ \text{quartile} - 2^{nd}\ \text{quartile}) * 1.5 \quad (2)$$

$$\text{High threshold} = 3^{rd}\ \text{quartile} + (3^{rd}\ \text{quartile} - 2^{nd}\ \text{quartile}) * 1.5 \quad (3)$$

3.3.2.2 Choose the optimal size of moving window

The first step of reconstruction in time is choosing the moving window's size, which is crucial to control the accuracy and percentage of filled pixels. Start by calculating the autocorrelation of LST for a series of increasing distances for the 16 downloaded Aqua/Terra scenes using the incremental spatial autocorrelation tool in ArcGIS pro software to ensure that all pixels inside the moving window are highly correlated. The associated distance with the peak spatial autocorrelation for each scene has been calculated, then calculating distances' mean value. Any moving window scale within the mean value is appropriate to use but with various percentages of filled pixels and accuracy. Therefore, to choose the optimal size within this scale, a block of valid pixels removed, then predict those removed pixels using different sizes of moving window to check the performance of moving window, then chose a size that balance between the percentage of filling pixels, accuracy, and computing work.

3.3.2.2 Fill the gaps using adjustment value

There are fluctuations of LST values during the day. Therefore, the observations in the morning tend to be cooler than afternoon [16]. Considering these differences in LST values between the overpasses by adding an adjustment value before filling the gaps [17]. The adjustment value has been estimated for each missing pixel separately by calculating the mean value of LST differences between Aqua and Terra overpasses inside a moving window centered above the missing pixel.

Figure 4 presents the step of filling the gap in time. The processes started with scanning the same pixel in Terra/Aqua with an odd-sized moving window, and if the central pixel is missing in one of the two scenes, it was filled by the same pixel's value from the other scene in addition to the adjustment value. When all the pixels around the central pixel are missing, then the pixel will not be filled even if the other LST scene's central pixel is valid because it will not be possible to calculate the adjustment value.

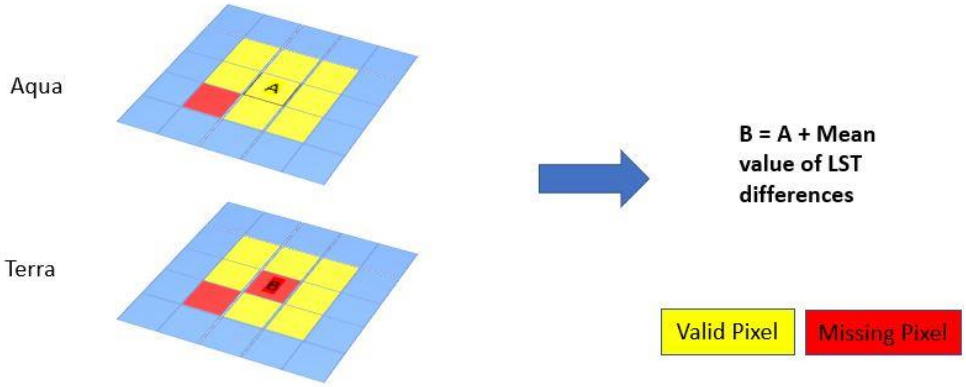

Figure 4. Reconstruct MODIS LST (Aqua and Terra) in time.

Here is an example of filling missing pixels in Aqua. Using a moving window of 3 * 3 size with simple numbers to simplify the processes. Let assumes the following matrices present the moving window from Aqua and Terra :

$$aqua = \begin{pmatrix} 15 & 16 & 12 \\ 13 & x & 12 \\ 13 & 14 & NA \end{pmatrix} \qquad terra = \begin{pmatrix} 18 & 17 & 35 \\ 14 & 15 & 12 \\ 15 & 15 & 11 \end{pmatrix}$$

The first step was calculating the differences between the valid pixels inside the moving window:

$$aqua - terra = \begin{pmatrix} -3 & -1 & -23 \\ -1 & x & 0 \\ -2 & -1 & - \end{pmatrix}$$

It could be seen from the differences that there is a big difference between two pixels reach to 23 °C; this difference indicates that one of the two pixels is an outlier, so it will be excluded from calculating the adjustment value, then calculate the mean value of differences to be the adjustment value by following:

$$adjustment\ value = \frac{(-3) + (-1) + (-1) + (-2) + (-1) + 0}{6} = -1.3$$

The missing pixel in Aqua (x) will be equal to 13.7 by adding the adjustment value to the same pixel's value in Terra. Here, the adjustment value was negative because the Terra LST was warmer than Aqua LST.

3.3.3 Reconstruction in space

3.3.3.1 Selection of best variables

Select the required variables to predict LST using the best subset method for downloading 16 Aqua/Terra scenes. The best subset method is applicable in this case because the number of independent variables is small, so the possible subsets are small, and the computational effort is not high [41]. The best subset method applies separated Ordinary Least Squares (OLS) regression for each possible combination of covariate variables to find the best subset selection of variables. Fit model for each predictor separately and finding the best one, then fit model for every two predictors and so forth, ends up to 2 ^ P models that P is the number of predictors [42]. Two different statistical tests were used to compare the best available models, Cp -statistic of Mallows and adjusted R2, to see the effect of adding variables to the model and know when the model fit starts to be stable [42].

3.3.3.2 Generalized Additive Models (GAM)

GAM is a nonparametric model deals with the non-linearity relationship between predictors and response variables [43]. GAM fitting the non-linearity of variables by smoothing terms, those terms retain as an additive structure of the linear model, which makes it easy to fit GAM using different smoothing functions like Thin Plate Spline or cubic spline smoothing [42], to get the model as the following equation:

$$Y_i = a_0 + f_1(X_{i1}) + \cdots + f_n(X_{in}) + \varepsilon_i \qquad (4)$$

Where (f) is a smoothing function for the prediction/covariate variables $(X_{i1}, \ldots, X_{in})$, a_0 is the intercept parameter, and ε_i is the residual component. Equation 4 was used to develop the GAM model for the 16 downloaded Aqua/Terra scenes by smoothing the most important covariate variables obtained from the previous step to determine how the percentage of missing pixels could affect the performance of GAM. Then, choose two scenes with almost the same percentage of missing pixels but the different distribution of spatial gaps to check the effect of the spatial distribution of gaps on the performance of GAM. Then, the interaction between the spatial location was used to build the spatial trend surface, and this interaction fitted using two-dimensional smoothing, then the model written as the following equation:

$$Y_i = a_0 + f_1(Lat_i, Long_i) + f_2(X_{i1}) + \cdots + f_n(X_{in}) + \varepsilon_i \qquad (5)$$

f_1 is the two-dimensional smoothing function for the spatial locations of LST pixels; adding this term helps the model consider the spatial structure of the data and improve the performance of the GAM model. The elevation added to the 2D spatial surface for building a more complex surface represents the geospatial data into the GAM model. That would improve the model and present the spatial trend precisely. Adding elevation required 3-dimensional smoothing, and elevation has a different scale than coordinates of spatial location, which required tensor product to model the 3-d smooth interaction [44]. The tensor product allows a choice of different smoothing parameters for each variable in the multidimensional interaction term [10] and separates the interaction of elevation with spatial locations from the individual effect of using the elevation. The model would be written as the following equation:

$$Y_i = a_0 + f_1(Lat_i, Long_i, Elevation_i) + f_2(X_{i1}) + \cdots + f_n(X_{in}) + \varepsilon_i \qquad (6)$$

f_1 is the three-dimensional smoothing function, and cubic regression spline represents the basis of the covariate variables (e.g., elevation, aspect, slope), thin plate regression splines to represent the spatial location of pixels. Those smoothing functions have a penalty term to find the optimal degree of freedom for the smoothing and avoid overfitting, so no need to apply cross-validation to find the variable's best smoothness [45,46].

3.3.4 Validation

Aqua daytime LST overpasses on 31 Oct 2016 used for the evaluation, the Aqua scene has 27% of missing pixels already, the validation was by making artificial gaps of different sizes in the scene, then predict them using the developed method and make a comparison between the predicted values and original values in the validated blocks. The process started by simulated 3% of gaps in different places to have 30% of missing pixels in total. The second validation was by adding 10% of an artificial gap to have 37% of missing pixels in total, then making 25% of an artificial gap to have 52% of missing pixels in total. Figure 5 shows the extent of the artificial gap by a different proportion of missing pixels.

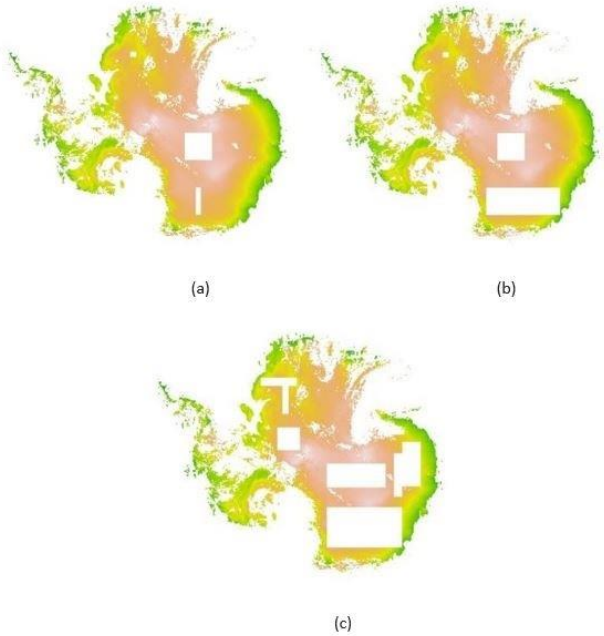

Figure 5. Artificial gaps of different sizes for Daytime LST scene (31 Oct 2016), (a) 3% of the artificial gap, (b) 10% of the artificial gap, (c) 25% of the artificial gap

3.3.5 Method comparison

A comparison between the developed method and a novel approach developed by Metz et al. [1] has been to see the developed method's performance compared with another exciting method used to fill gaps in the MODIS LST dataset. Metz et al. [1] used Local Weighted Regression (LWR) to fill gaps in time using a time series of 14 images, then fill the remaining gaps in space using Thin Plate Spline (TPS) interpolation with covariates (DEM and emissivity). The previously validated blocks have been predicted again using Metz et al. approach, then comparing the new results (Metz et al.) and the old results (The developed method).

4 Results

This section presents data processing results and the applied methods to fill the gaps. Included the results of filling in time, filling in space, validation processes, and comparing another approach of filling the gaps.

4.1 Exploratory data analysis

A correlation matrix between the variables (Figure 18 in the Appendix) was checked to avoid collinearity between variables. It showed that terrain Ruggedness Index, roughness, and slope are highly positively correlated (0.99). Therefore, one variable is enough to use; the slope has been selected to use in the next steps. Table 1 shows the final six predictors of LST used in this study. Table 2 shows the percentage of missing pixels among the different 16 scenes used in this study.

Table 1. The six predictors for LST in Antarctica

Predictor	Predictor
Elevation	TPI
Slope	Emissivity
Aspect	Solar incidence angle

Table 2. Percentage of missing pixels for different Aqua/Tera scenes in 2016.

Date	Missing pixels - Aqua		Missing pixels - Terra	
	Daytime	Nighttime	Daytime	Nighttime
15 Jan	30%	16%	19%	16%
30 March	13%	24%	9%	26%
15 Sep	18%	29%	8%	36%
31 Oct	27%	21%	8%	12%

4.2 Reconstruction in time

4.2.1 Filter unreliable values of LST

First, the Terra scene was subtracted from the Aqua scene to check the LST differences (Figure 6). It could be seen that there are pixels with very high differences, which is more than 40 oC within just 3 hours. A quantile outlier detector was then used to detect those pixels to exclude them from calculating the adjustment value. Figure 7 shows the LST differences after excluding the pixels that have an extreme change of LST values.

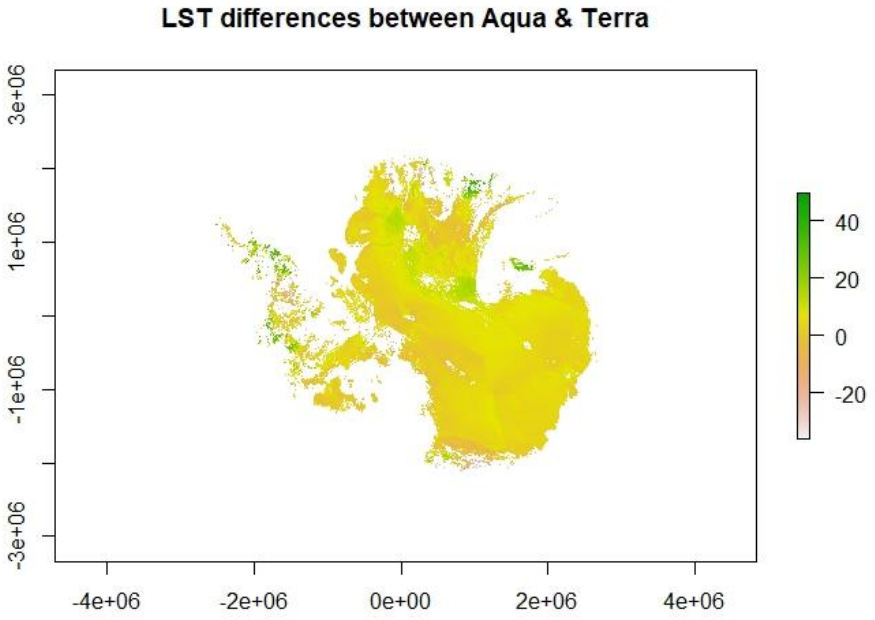

Figure 6. LST differences between daytime Aqua and Terra LST (31 Oct 2016).

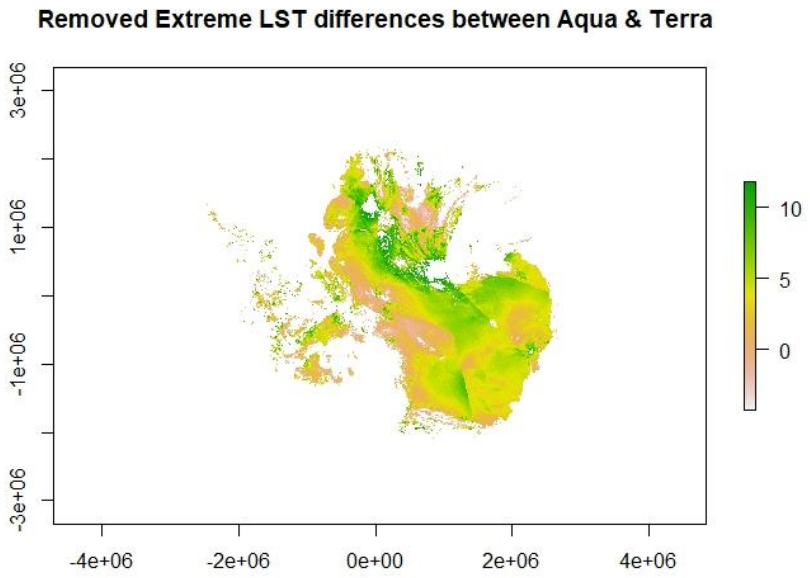

Figure 7. LST differences between daytime Aqua and Terra after deleting extreme differences (31 Oct 2016).

4.2.2 Choose the optimal size of the moving window

Figure 8 explains spatial autocorrelation measurement for a series of distances for the Daytime Aqua scene (15 Sep 2016). These results show us how the LST values were clustered within different distances, and the z-score reflects the intensity of spatial clustering associated with distances. The autocorrelation (clustering) increased with increasing the distance to reach the peak at a certain distance then started to go down again, which means all the pixels within the peak distance are highly correlated. Therefore, any moving window scale within the peak distance would be an appropriate scale for the moving window.

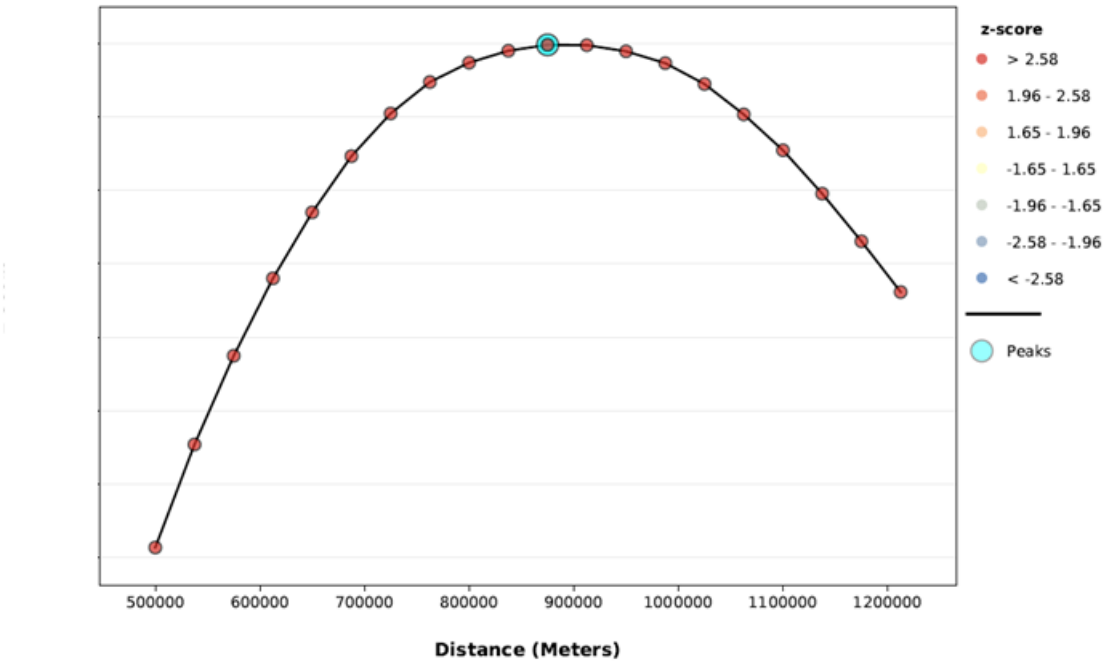

Figure 8. Spatial Autocorrelation by Distance, for Aqua's 1:30 pm overpass (15 Sep 2016).

Table 3 shows the maximum distance associated with the peak spatial autocorrelation for each downloaded Aqua/Terra scene. It was noticed that the associated distances with the peak spatial autocorrelation were almost stable in all scenes, ranging between 950 and 1200 km. The mean value of maximum distances was 1100 km among different scenes, then any scale of moving window within this distance could be used to fill the gaps.

Table 3. Distance threshold for the maximum spatial autocorrelation for different MODIS LST scenes observed by Aqua in 2016, associated with the percentage of missing pixels in each scene.

Date	Distance Threshold Aqua		Distance Threshold Terra	
	Daytime	Nighttime	Daytime	Nighttime
15 Jan	950	1250	1175	1250
30 March	1150	1150	1150	1150
15 Sep	1175	875	1250	1050
31 Oct	1137	1250	1140	1250

4.2.2 Fill the gaps using adjustment value

Table 4 and Table 5 indicates that there are fluctuations of LST values during the daytime/nighttime. In general, the night overpasses are colder than day overpasses. The coldest LST was in winter (September) by average -48.14 ^{o}C during the day and -51.73 ^{o}C during the night, while the hottest LST was in summer (January) by average -21.93 ^{o}C during the day and -27.30 ^{o}C during the night. A comparison between Terra and Aqua's LST values shows that LST values for Terra are warmer than Aqua's observation by an average of 0.5 ^{o}C. These facts prove the importance of adding adjustment value to the LST values before filling the target scene.

Table 4. Mean values of LST observations from Terra and Aqua during the day for different scenes in 2016.

Date	Mean LST (10:30 AM, Aqua) (Celsius)	Mean LST (1:30 PM, Terra) (Celsius)
15 Jan	-19.53	-24.33
30 March	-43.15	-43.67
15 Sep	-47.48	-48.80
31 October	-33.92	-38.46

Table 5. Mean values of LST observations from Terra and Aqua during the night for different scenes in 2016.

Date	Mean LST (22:30 PM, Aqua) (Celsius)	Mean LST (13:30 AM, Terra) (Celsius)
15 Jan	-26.61	-27.98
30 March	-45.89	-46.73
15 Sep	-51.35	-52.11
31 October	-39.41	-41.76

LST differences between Aqua and Terra were different among the study area. In some places, the difference is small while it is significant in other areas, therefore using a global adjustment value for all pixels does not make sense. The adjustment value changed among the study area using the moving window to include just the correlated pixels inside the window for calculating the adjustment value.

As mentioned in the previous step, any size of moving window within the scale of 1100 km would be right to fill the gaps. Different moving windows were used to predict a deleted block of valid pixels (50,000 pixels) to find the optimal size. The small moving window (3*3) filled 1% of the deleted block, then 25 * 25 filled 27%, the larger window (49 * 49) filled more pixels by 52% of the deleted block. Increasing the moving window size increased the number of filled pixels, but that affects the accuracy of predictions and computing work. Figure 9 presents a comparison between original and predicted LST values using the different moving window, increasing the moving window's size increased the number of outliers, and increased the range of predicted values.

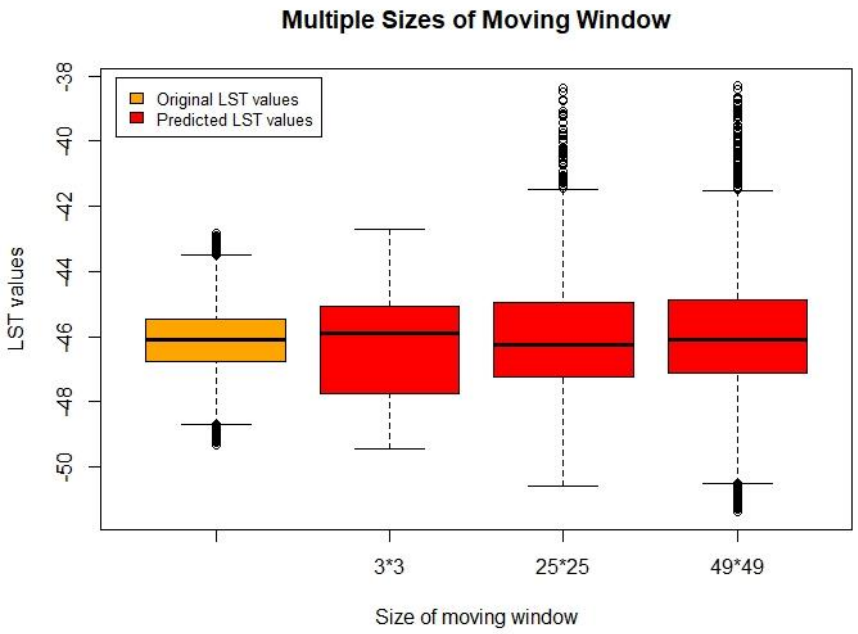

Figure 9. Comparison between predicted values using different sizes of moving window.

In this study, a moving window of size 47 by 47 (the area approximating 2,210 km2) has been selected to trade between the number of filled pixels, the accuracy of filled pixels, and the computational work. 48% of Aqua's missing pixels were filled using a 47 * 47 moving window size (Figure 10).

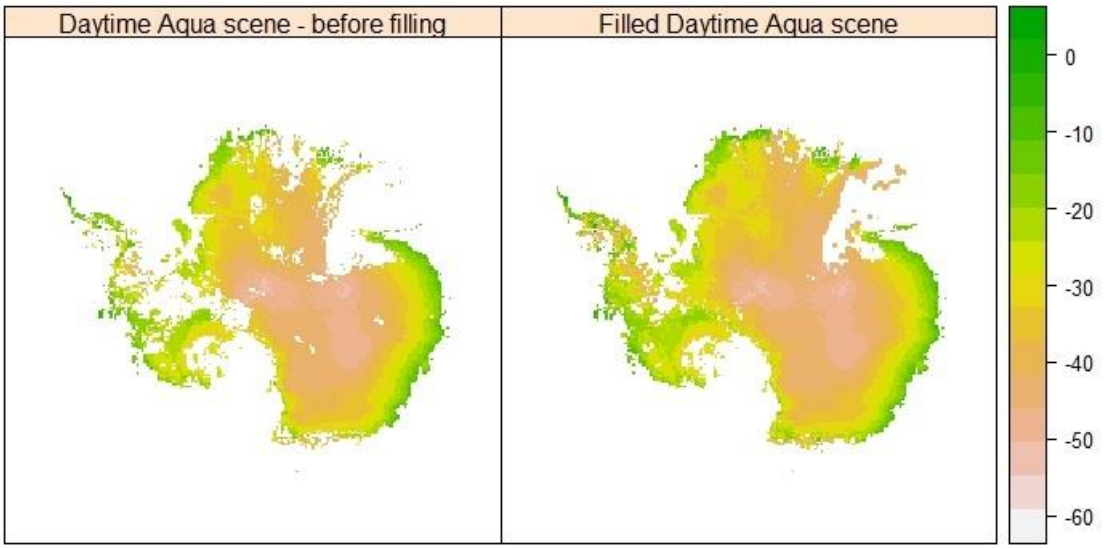

(a) *(b)*

Figure 10. Aqua day's overpass (31 Oct 2016), (a) before filling and (b) after filling.

4.3 Reconstruction in space

4.3.1 Best subset regression

The best subset method was used to find the most important variables to predict LST in Antarctica and tested for the 16 downloaded scenes. It found that there were six best models, it could be seen that the best one variable model contains only the elevation, and the best 2-variables model contains just the elevation and the aspect, and so forth (Table 6).

Table 6. Best models to predict LST values.

Best Models	Variables
1-variable model	elevation
2-variables model	+ Aspect
3-variables model	+ Slope
4-variables model	+ Emissivity
5-variables model	+ TPI
6-variables model	+ Solar Incidence angle

Two statistical metrics were used to compare the models' performance to choose the best model among the six models. Figure 11 shows Mallows' Cp statistic test for the Aqua scene's six models on 31 Oct 2016. It could be seen that the most significant improvement was by adding the aspect to the model, then adding more variables improved the model a little bit. Because Mallows' Cp value started to decrease slightly after adding more than two variables, it could not be possible to say that the six variables model is better than the two variables model.

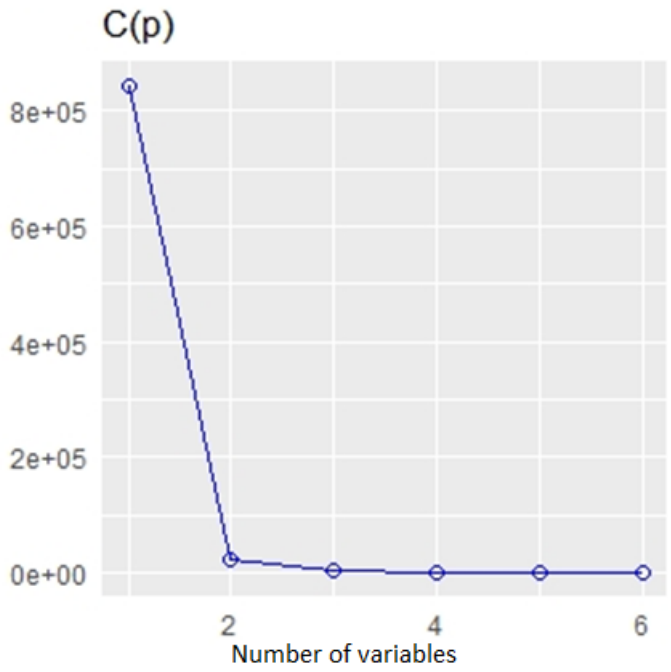

Figure 11. Mallows' Cp for a model by adding variable each time for daytime Aqua LST scene (31 Oct 2016).

The second statistical test was adjusted R2 (Table 7), the Adj. R2 for the one-variable model was 0.51, then improved to be 0.52 after adding aspect to the model, then it can be noticed that the model was stable when adding more variables to the model. Mallows' Cp and Adjusted R2 were used to test models for all downloaded Aqua/Terra scenes from the four different dates. There was a significant improvement when adding the aspect to the model and sometimes a small improvement. In general, the models behave in the same way, and they were improved when adding the aspect then stay stable.

Mainly, terrain-related variables represented by the elevation and the aspect were the most important variables to predict LST in Antarctica. Previous works suggested using an emissivity band to improve the results taking advantage of the

contrast between land covers, but according to land cover classification for Antarctica based on a 1:100000 scale, there are three land cover classes: ice-free rocks, blue ice, and snow [47]. The three classes have almost the same emissivity values, which would explain why the emissivity band was not essential to fill MODIS LST gaps in Antarctica.

Table 7. Adjusted R2 for the best six models for daytime Aqua LST scene (31 Oct 2016).

# of variables for the model	Adj. R2
1 (Elevation)	0.51
2 (+ Aspect)	0.52
3 (+ Slope)	0.52
4 (+ TPI)	0.52
5 (+ Emissivity)	0.52
6 (+ Solar incidence angle)	0.52

4.3.2 Generalized Additive Model (GAM)

Terrain-related variables (elevation and aspect) were used to build a GAM using the available valid pixels in each Aqua/Terra scene. Cubic spline smoothing was used to smooth the variables with an internal penalty to find the best smoothing and avoid overfitting. Table 8 and Table 9 show the Adj. R2 for the different GAM models to find out if there is any relation between the percentage of missing pixels and the performance of GAM, the results show that the models with a high percentage of missing pixels vary between high and low Adj. R2, and that is the same for the models with a low percentage of missing pixels.

Table 8. Adjusted R2 for GAM models for different day/night Aqua scenes.

Date	Missing pixels	Adj. R2
15 Jan - Day	30%	0.88
15 Jan - Night	16%	0.76
30 Mar - Day	13%	0.52
30 Mar - Night	24%	0.61
15 Sep - Day	18%	0.69
15 Sep - Night	29%	0.67
31 Oct - Day	27%	0.64
31 Oct - Night	21%	0.63

Table 9. Adjusted R2 for GAM models for different day/night Terra scenes.

Date	Missing pixels	Adj. R2
15 Jan - Day	19%	0.82
15 Jan - Night	16%	0.81
30 Mar - Day	09%	0.55
30 Mar - Night	26%	0.60
15 Sep - Day	08%	0.65
15 Sep - Night	36%	0.67
31 Oct - Day	08%	0.54
31 Oct - Night	12%	0.58

Two Aqua scenes (Figure 12) were used to study the effect of the spatial configuration of gaps on GAM performance, the two different scenes have almost the same percentage of missing pixels, but the clouds cover was taking different sizes and distribution. The gaps in the first scene (15 Jan 2016) centered in the middle of the scene with continuous gaps, while the gaps in the second scene (31 Oct 2016) were distributed around the border of the scene and in small sizes, that would affect the smoothing function mainly at the border. Figure 13 shows how the smoothing function looks different for the two scenes even they have almost the same percentage of missing pixels, and the smoothing function was wigglier for the Aqua scene (31 Oct 2016), that explains why the fitted GAM of the Aqua scene (15 Jan 2016) with 0.88 of Adj. R2 was better than GAM of Aqua scene(31 Oct 2016) with 0.64 pf Adj. R2.

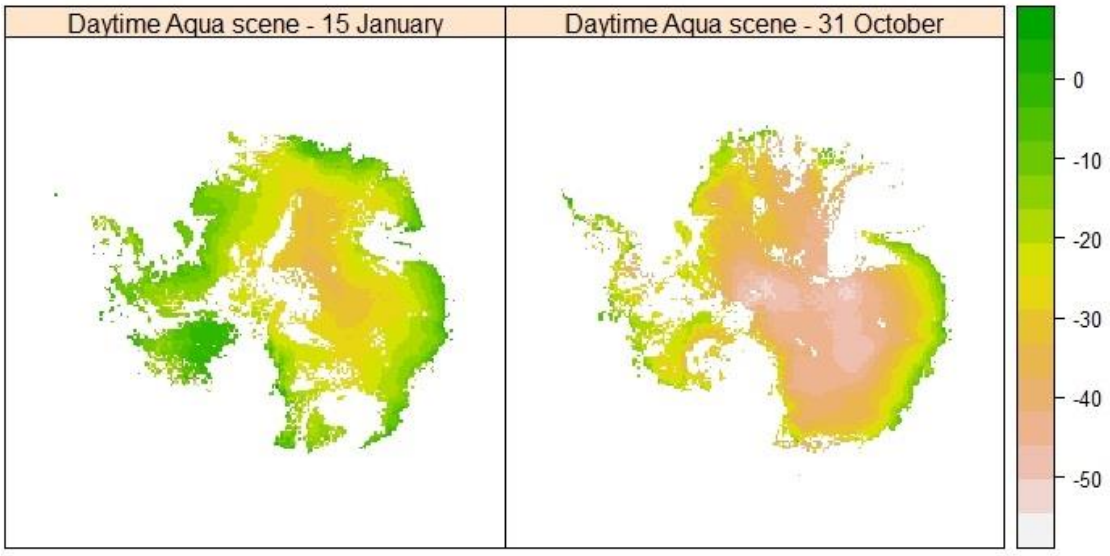

Figure 12. Aqua day scenes observed in 2016, percentage of missing pixels on 15 Jan is 30%, and on 31 Oct scene is 27%.

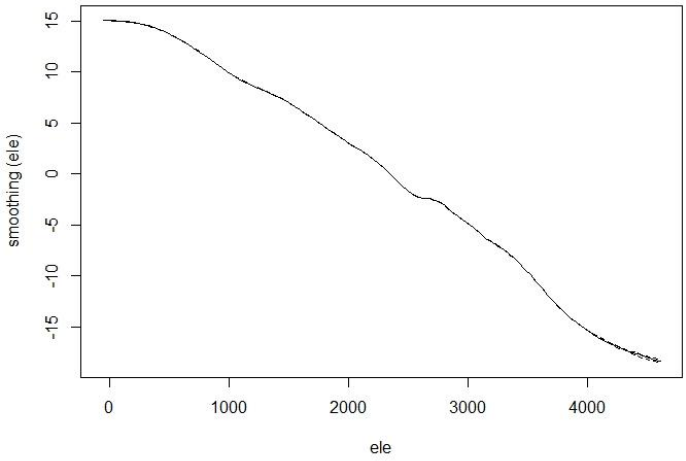

(a)

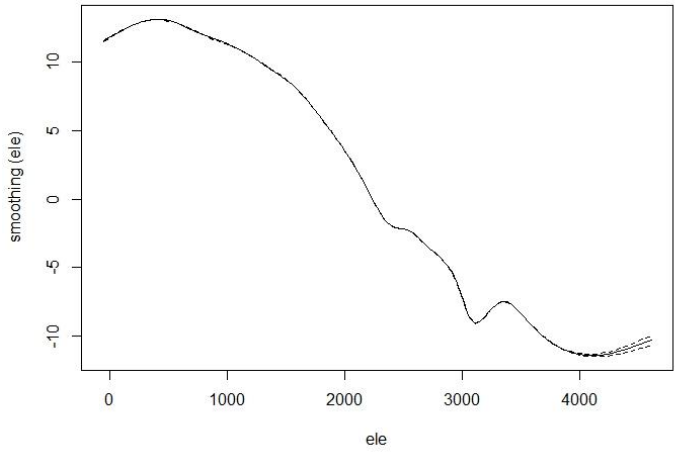

(b)

Figure 13. Smoothing function, (a) Aqua scene (15 Jan 2016), (b) Aqua scene (31 Oct 2016).

4.3.2.1 GAM with a 2D spatial trend

In this section, the GAM model was extended by adding spatial surface using smoothing interaction between the spatial locations of valid pixels; to represent the spatial structure in the model and improve the goodness of fit GAM model. Table 10 and Table 11 show the adjusted R2 for GAM models fitted on the available valid pixels in the 16 downloaded Aqua/Terra scenes.

Table 10. Adjusted R2 and AIC for GAM models with 2D spatial trend surface for different Aqua day/night scenes.

Date	Aqua Day		Aqua Night	
	Adj. R2	AIC	Adj. R2	AIC
15 Jan	0.93	38303763	0.86	55459246
30 March	0.84	63261149	0.88	52612317
15 Sep	0.88	56625321	0.86	48047266
31 Oct	0.86	48684822	0.82	55659608

Table 11. Adjusted R2 and AIC for GAM models with 2D spatial trend surface for different Aqua day/night scenes.

Date	Terra Day		Terra Night	
	Adj. R2	AIC	Adj. R2	AIC
15 Jan	0.85	51969809	0.88	54044856
30 March	0.84	68017916	0.87	51618657
15 Sep	0.84	66160541	0.88	41868328
31 Oct	0.76	68966194	0.75	64956140

4.3.2.2 GAM with a 3D spatial trend

Table 12 and Table 13 shows the influence of adding elevation to the spatial trend using tensor smoothing. The model fit improved in all cases of adding 3-dimensional spatial surface, adjusted R2 increased while AIC decreased, which indicates that the model fit improved.

Table 12. Adjusted R2 and AIC for GAM models with 3D spatial trend surface for different Aqua day/night scenes (2016).

Date	Aqua Day		Aqua Night	
	Adj. R2	AIC	Adj. R2	AIC
15 Jan	0.94	36045215	0.91	50778017
30 March	0.90	57969597	0.93	46782604
15 Sep	0.91	54441963	0.88	46888808
31 Oct	0.91	45338474	0.87	52420050

Table 13. Adjusted R2 and AIC for GAM models with 3D spatial trend surface for different Terra day/night scenes (2016).

Date	Terra Day		Terra Night	
	Adj. R2	AIC	Adj. R2	AIC
15 Jan	0.90	47642558	0.93	49252035
30 March	0.89	63196099	0.93	46012063
15 Sep	0.88	62806345	0.90	40464175
31 Oct	0.81	66495490	0.82	61653801

In the following, GAM with a 3D spatial surface was used to fill the remaining gaps in the Aqua scene (31 Oct 2016). Fig. 14 presents the GAM smoothers of the included covariate variables (elevation and aspect). The plots confirm that the relationship between LST and the elevation was non-linear, but the relation with the aspect was linear, so no need to smooth it anymore, and that would help reduce the computational work of GAM.

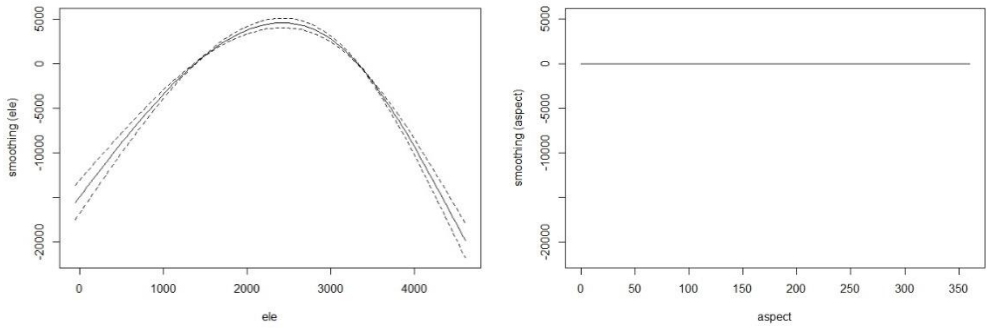

Figure 14. GAM smoothers of elevation and aspect when adding 3D spatial surface to GAM.

Figure 15 presents the diagnostic plots of the GAM model, the residuals centered to zero, and there is a strong relationship between fitted value and response. The histogram of residuals shows a normal distribution of residuals. The relation between predictions and residuals shows some output with extreme residuals, which is an indicator of outliers' presence, and include them in the analysis would affect GAM fit and the results. Figure 16 shows the final scene after filling the remaining gap using GAM with a 3-dimensional spatial surface.

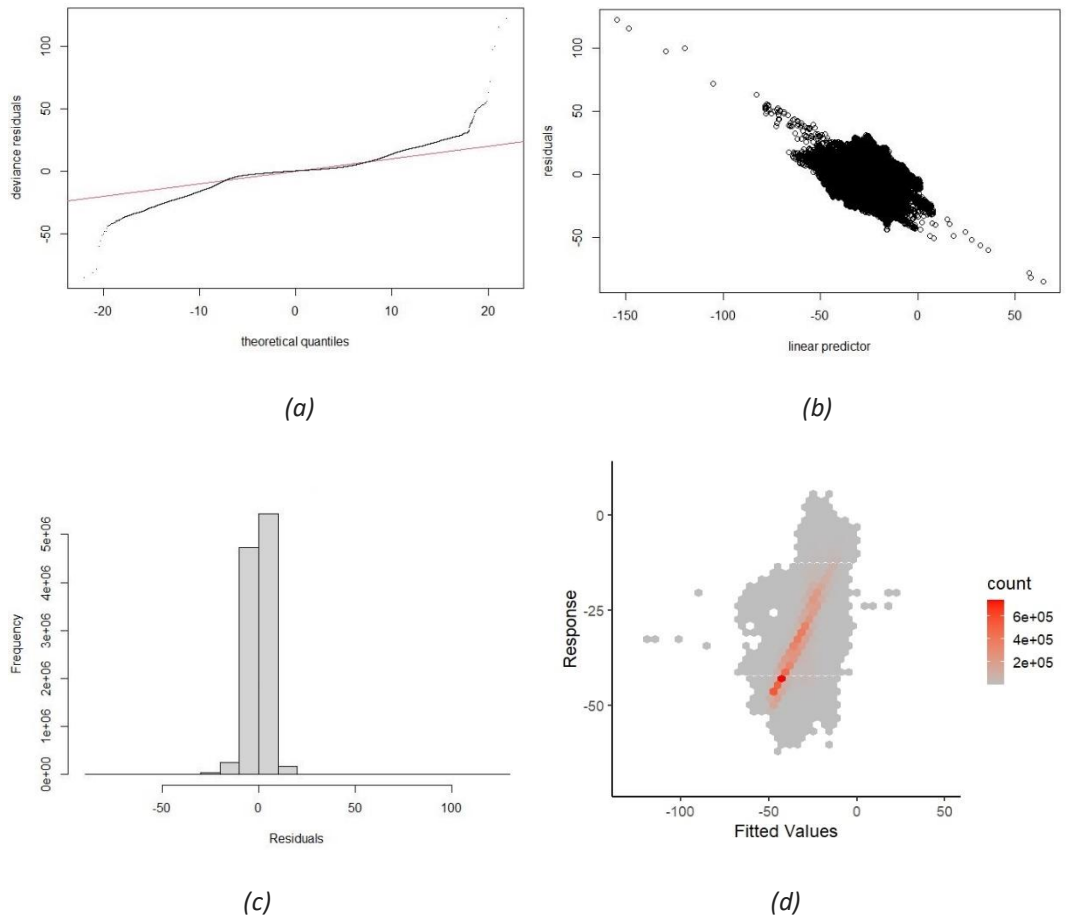

Figure 15. Diagnostic plots of GAM, (a) Normal Q-Q, (b) Residuals vs linear predictions, (c) Histogram of residuals, (d) Response vs Fitted Values.

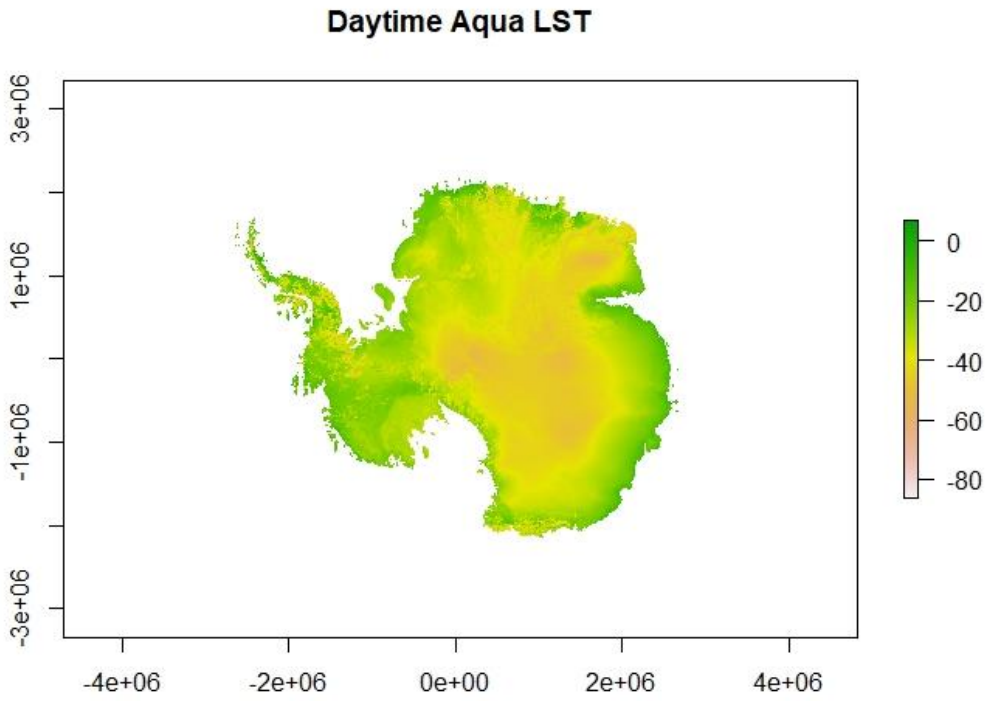

Figure 16. Daytime LST (31 Oct 2016), after fill the remaining gap using GAM with the 3-dimensional spatial surface.

4.4 Validation

As mentioned in the previous section, the percentage of missing pixels and the spatial distribution of gaps affect the performance of GAM. Therefore, the reconstruction method was validated by creating artificial gaps of different sizes and places in the original MODIS LST data, then refill those gaps. Table 14 shows the values of RMSE and R2 for the different percentages of artificial gaps, while Figure 17 shows the distribution of original LST values in the validated blocks.

For 3% of artificial gaps, the predicted LST values deviated by 0.72°C from the original LST values with R2 equal to 0.98, and the mean value of original LST was -44.60°C with a standard deviation of 3.42 °C. The RMSE increased to 1.70 with 0.96 of R2 while increasing the artificial gaps to 10%. The highest RMSE was 2.91 with 0.87 of R2 when simulated 25% of artificial gaps, while the mean value of original LST was -38.39°C with a standard deviation of 6.51 °C. The resulting RMSE values were low for the different artificial gaps concerning the mean and the standard deviation of original LST values in the validated blocks.

Table 14. Evaluation of the artificial gap's reconstruction using RMSE and R2.

Artificial gaps	Total gaps	RMSE	R2	Mean	Standard deviation
3%	30%	0.72	0.98	-44.60	3.42
10%	37%	1.70	0.96	-38.70	6.65
25%	52%	2.91	0.87	-38.39	6.51

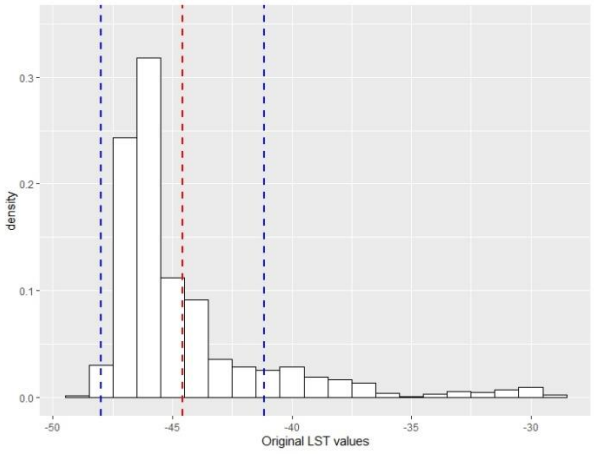

(a)

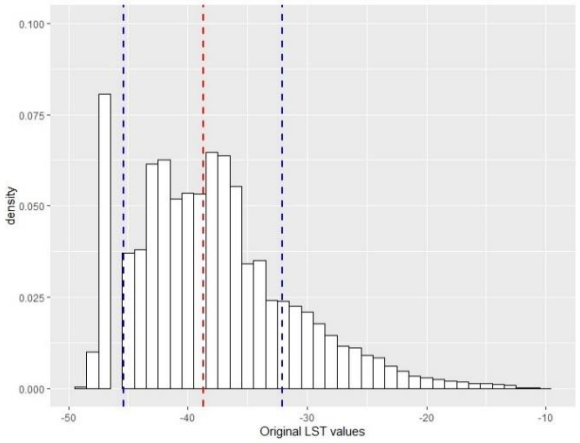

(b)

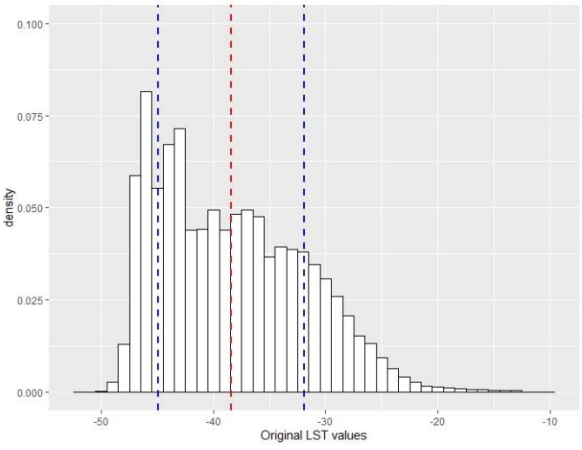

(C)

Figure 17. Distribution of original LST values in the simulated gap, (a) 3% of the artificial gap, (b) 10% of the artificial gap, (c) 25% of the artificial gap.

4.5 Method comparison

The validated blocks in the previous step have been predicted using the method employed by Metz et al. [1], then compare the new results with the results of the developed method. Table 15 shows the values of RMSE and R2 for the two methods. The predictions of the developed method were better for 3% and 10% of artificial gaps. However, when increasing the artificial gaps to 25%, the method adopted by Metz et al. was better at taking advantage of using 14 images in time, which help fill more pixels in time and improve the second part of spatial interpolation. In this case, increasing the size of the moving window to 125 * 125 in the temporal part of the developed method helped to fill more pixels, then decreasing the gaps in space and improve the spatial trend surface to improve the overall accuracy and decrease the RMSE value to 2.27 with 0.92 of R2.

Table 15. Comparison between reconstruction methods for different artificial gaps.

Artificial gaps	The Developed method		Method of Metz et al. 2017	
	RMSE	R2	RMSE	R2
3%	0.72	0.98	1.89	0.75
10%	1.70	0.96	1.80	0.93
25%	2.91	0.87	2.32	0.89

5 Discussion

5.1 Findings

This research presented a flexible method to fill the gaps in MODIS LST data. The method relies on low processing time by using just one scene in time, use the most efficient predictors, and let the user balance between prediction accuracy and run-time based on his research needs instead of using high mathematically computing work.

The temporal approach of gap-filling of MODIS LST data mainly relies on the percentage of valid pixels in the reference scene and the moving window's size. A large moving window fills more gaps in MODIS LST data but less accuracy and high computing work, while a smaller moving window fills fewer gaps with less computing work and high accuracy. Any moving window scale within 1100 km distance is right to use for Antarctica, but the standard size is 47 * 47 to balance the number of filling pixels, the accuracy of predictions, and computing work.

Terrain-related variables (elevation and aspect) are the best variables to predict LST in Antarctica. The results showed that the emissivity band does not substantially impact the prediction of LST in Antarctica because Antarctica's land cover classes at the scale of 1 Km have almost the same emissivity values. GAM is an excellent approach to present the spatial part of this method because of its ability to deal with non-linear relationships between variables. Also, it is easy to apply a smoothing function on the interaction between variables, which allows adding 2-dimensional spatial trend using the spatial location, which leads to improving the performance of GAM by presenting the spatial autocorrelation among the data.

The 2D spatial surface extended to the 3D surface by adding elevation to the interaction between spatial locations. 3-dimensional spatial surface improved the fit of GAM and gave better results but increased the computational work to build the model. The results showed that the performance of GAM was affected by the percentage of missing pixels and the spatial distribution of gaps somehow by affecting the behavior of the smoothing function.

The developed method performed better for small gaps and made more accurate predictions of LST. The results showed that the newly developed method outperformed LWR + TPS method used by Metz et al.[1] when the scene has a low percentage of missing pixels. However, both methods gave results slightly closed to each other when the percentage of missing pixels is very high.

This approach fills the gaps in time and then fills the remaining gaps in space, which is better than filling in space and filling in time. That is because there are scenes with a low percentage of valid pixels to apply spatial interpolation. Starting by filling the gaps in time reduces the gaps and increases the percentage of valid pixels, which improves the spatial interpolation part. On the other hand, that would increase the dataset's noise because of increasing the dataset size. In the developed method, starting by filling in time provides more valid pixels, improving the spatial interpolation part by capturing more details in the empty areas and improving the overall accuracy.

5.2 Limitations and Future work

The smoothing function in the GAM model is affected by the noise in the dataset, and increasing the valid pixels in the temporal part and using all the valid pixels increases the dataset's noise. Future work to reduce the noise in the dataset, like bootstrap sampling combined with the ensemble learning approach with GAM as the base model, would help reduce the noise and make the processing time of building the model faster and more efficient using smaller dataset.

This research focused on filling the pixels with no LST values due to clouds. However, there are pixels with high LST error, and the algorithm of cloud detection in MODIS data failed to detect thin clouds [7,8], which means that there are pixels that have unreliable LST values (outliers) included in the method of filling the gaps, that would lead to an unusual pattern in some areas of the final product of MODIS LST scene. Future work to detect unreliable pixels, predict them, and assign them with new reasonable and reliable LST values.

The performance of GAM affected by the percentage of missing pixels, but this study used 16 scenes downloaded from four different dates, and that was not enough to find the relation between the percentage of missing pixels and the performance of GAM. Another factor needs more investigation to find out how could affect the performance of GAM is the spatial distribution of gaps, and this would help to use different smoothing function for different scenes based on the spatial distribution of gaps.

One scene used in the validation process to check the developed method's performance, future work to check the method's performance on multiple scenes would help check the stability of predictions and uncertainty.

6 Conclusion

This research presents a newly developed method of filling gaps in MODIS LST data using temporal and spatial information. The new method provides highly accurate results with low processing time using just one reference image instead of long time-series of images with an adaptive moving window defined and use parallel computing to build GAM and 3D spatial trend surface.

The method starts by filling the gaps partially in time using the nearest scene on the same day by a moving window; increasing the moving window size controls the percentage of filling pixels and accuracy of predictions by filling more pixels but with less accuracy. In Antarctica, a moving window of 47 * 47 size is a good one to use, but it is more efficient to use a bigger moving window when the scene has a very high percentage of gap (> 50%). The remaining gaps filled in space by building a two-variables GAM model contains only the elevation and the aspect, which is the best model to predict LST in Antarctica, then add 3D spatial trend surface (spatial location and elevation) to GAM to improve the results.

The developed approach has a more excellent predictive capability (with a percentage of gaps < 40%) than other spatio-temporal approaches, while it has less predictive capability under a higher percentage of cloud cover. Future work still needed to reduce the noise in the dataset, detect unreliable LST values, and check the method's performance under different spatial distribution conditions of gaps and percentage of missing pixels to find out the best smoothing function for different conditions.

The developed method implemented into R package (https://masawdah.github.io/modislst) with user-defined options for the size of moving window, covariate variables, smoothing function, spatial surface. Therefore, it could be used for any other study area.

References

[1] Metz, M., Andreo, V., & Neteler, M. (2017). A new fully gap-free time series of land surface temperature from MODIS LST data. Remote sensing, 9(12), 1333.

[2] Metz, M., Rocchini, D., & Neteler, M. (2014). Surface temperatures at the continental scale: tracking changes with remote sensing at unprecedented detail. Remote Sensing, 6(5), 3822-3840.

[3] Weng, Q. Thermal infrared remote sensing for urban climate and environmental studies: Methods, applications, and trends. ISPRS J. Photogramm. Remote Sens. 2009, 64, 335–344.

[4] Wang, M., He, G., Zhang, Z., Wang, G., Zhang, Z., Cao, X., ... & Liu, X. (2017). Comparison of spatial interpolation and regression analysis models for an estimation of monthly near surface air temperature in China. Remote Sensing, 9(12), 1278.

[5] Stahl, K., Moore, R. D., Floyer, J. A., Asplin, M. G., & McKendry, I. G. (2006). Comparison of approaches for spatial interpolation of daily air temperature in a large region with complex topography and highly variable station density. Agricultural and forest meteorology, 139(3-4), 224-236.

[6] Meyer, H., Katurji, M., Appelhans, T., Müller, M. U., Nauss, T., Roudier, P., & Zawar-Reza, P. (2016). Mapping daily air temperature for Antarctica based on MODIS LST. Remote Sensing, 8(9), 732.

[7] Neteler, M. (2010). Estimating daily land surface temperatures in mountainous environments by reconstructed MODIS LST data. Remote sensing, 2(1), 333-351.

[8] Pede, T., & Mountrakis, G. (2018). An empirical comparison of interpolation methods for MODIS 8-day land surface temperature composites across the conterminous Unites States. ISPRS Journal of Photogrammetry and Remote Sensing, 142, 137-150.

[9] Tang, B., Bi, Y., Li, Z. L., & Xia, J. (2008). Generalized split-window algorithm for estimate of land surface temperature from Chinese geostationary FengYun meteorological satellite (FY-2C) data. Sensors, 8(2), 933-951.

[10] Poggio, L., Gimona, A., & Brown, I. (2012). Spatio-temporal MODIS EVI gap filling under cloud cover: An example in Scotland. ISPRS journal of photogrammetry and remote sensing, 72, 56-72.

[11] Williamson, S. N., Hik, D. S., Gamon, J. A., Kavanaugh, J. L., & Koh, S. (2013). Evaluating cloud contamination in clear-sky MODIS Terra daytime land surface temperatures using ground-based meteorology station observations. Journal of climate, 26(5), 1551-1560.

[12] Ghafarian Malamiri, H. R., Rousta, I., Olafsson, H., Zare, H., & Zhang, H. (2018). Gap-Filling of MODIS time series land surface temperature (LST) products using singular spectrum analysis (SSA). Atmosphere, 9(9), 334.

[13] Zhang, Q., Yuan, Q., Zeng, C., Li, X., & Wei, Y. (2018). Missing data reconstruction in remote sensing image with a unified spatial–temporal–spectral deep convolutional neural network. IEEE Transactions on Geoscience and Remote Sensing, 56(8), 4274-4288.

[14] Pede, T., & Mountrakis, G. (2018). An empirical comparison of interpolation methods for MODIS 8-day land surface temperature composites across the conterminous Unites States. ISPRS Journal of Photogrammetry and Remote Sensing, 142, 137-150.

[15] Scharlemann, J. P., Benz, D., Hay, S. I., Purse, B. V., Tatem, A. J., Wint, G. W., & Rogers, D. J. (2008). Global data for ecology and epidemiology: a novel algorithm for temporal Fourier processing MODIS data. PloS one, 3(1), e1408.

[16] Coops, N. C., Duro, D. C., Wulder, M. A., & Han, T. (2007). Estimating afternoon MODIS land surface temperatures (LST) based on morning MODIS overpass, location and elevation information. International Journal of Remote Sensing, 28(10), 2391-2396.

[17] Crosson, W. L., Al-Hamdan, M. Z., Hemmings, S. N., & Wade, G. M. (2012). A daily merged MODIS –Terra land surface temperature data set for the conterminous United States. Remote Sensing of Environment, 119, 315-324.

[18] Cresson, R., Ienco, D., Gaetano, R., Ose, K., & Minh, D. H. T. (2019, July). Optical image gap filling using deep convolutional autoencoder from optical and radar images. In IGARSS 2019-2019 IEEE International Geoscience and Remote Sensing Symposium (pp. 218-221). IEEE.

[19] Xu, Y., & Shen, Y. (2013). Reconstruction of the land surface temperature time series using harmonic analysis. Computers & geosciences, 61, 126-132.

[20] Yu, W., Nan, Z., Wang, Z., Chen, H., Wu, T., & Zhao, L. (2015). An effective interpolation method for MODIS land surface temperature on the Qinghai–Tibet Plateau. IEEE Journal of Selected Topics in Applied Earth Observations and Remote Sensing, 8(9), 4539-4550.

[21] Ke, L., Song, C., & Ding, X. (2012, July). Reconstructing complete modis lst based on temperature gradients in Northeastern Qinghai-Tibet Plateau. In 2012 IEEE International Geoscience and Remote Sensing Symposium (pp. 3505-3508). IEEE.

[22] Yu, W., Nan, Z., Wang, Z., Chen, H., Wu, T., & Zhao, L. (2015). An effective interpolation method for MODIS land surface temperature on the Qinghai–Tibet Plateau. IEEE Journal of Selected Topics in Applied Earth Observations and Remote Sensing, 8(9), 4539-4550.

[23] Galletti, C. S., Li, X., & Connors, J. P. (2019). Establishing the relationship between urban land-cover configuration and night time land-surface temperature using spatial regression. International Journal of Remote Sensing, 40(17), 6752-6774.

[24] Hengl, T., Heuvelink, G. B., Tadić, M. P., & Pebesma, E. J. (2012). Spatio-temporal prediction of daily temperatures using time-series of MODIS LST images. Theoretical and applied climatology, 107(1-2), 265-277.

[25] Song, J., Du, S., Feng, X., & Guo, L. (2014). The relationships between landscape compositions and land surface temperature: Quantifying their resolution sensitivity with spatial regression models. Landscape and Urban Planning, 123, 145-157.

[26] Chang, N. B., Bai, K., & Chen, C. F. (2015). Smart information reconstruction via time-space-spectrum continuum for cloud removal in satellite images. IEEE Journal of Selected Topics in Applied Earth Observations and Remote Sensing, 8(5), 1898-1912.

[27] Zhang, Q., Yuan, Q., Zeng, C., Li, X., & Wei, Y. (2018). Missing data reconstruction in remote sensing image with a unified spatial–temporal–spectral deep convolutional neural network. IEEE Transactions on Geoscience and Remote Sensing, 56(8), 4274-4288.

[28] Bromwich, D. H., Nicolas, J. P., Monaghan, A. J., Lazzara, M. A., Keller, L. M., Weidner, G. A., & Wilson, A. B. (2013). Central West Antarctica among the most rapidly warming regions on Earth. Nature Geoscience, 6(2), 139-145.

[29] Comiso, J. C., Gersten, R. A., Stock, L. V., Turner, J., Perez, G. J., & Cho, K. (2017). Positive trend in the Antarctic sea ice cover and associated changes in surface temperature. Journal of Climate, 30(6), 2251-2267.

[30] Miliaresis, G. C. (2014). Spatiotemporal patterns of land surface temperature of Antarctica from MODIS monthly LST (MYD11C3) data. Journal of Spatial Science, 59(1), 157-166.

[31] Retamales-Muñoz, G., Durán-Alarcón, C., & Mattar, C. (2019). Recent land surface temperature patterns in Antarctica using satellite and reanalysis data. Journal of South American Earth Sciences, 95, 102304.

[32] Bindschadler, R., Vornberger, P., Fleming, A., Fox, A., Mullins, J., Binnie, D., Paulson, S., Granneman, B., and Gorodetzky, D., 2008, The Landsat Image Mosaic of Antarctica, Remote Sensing of Environment, 112, pp. 4214-4226.

[33] https://lpdaac.usgs.gov/ WEBSITE

[34] https://ladsweb.modaps.eosdis.nasa.gov/

[35] Wan, Z. (2013). MODIS land surface temperature products users' guide. Institute for Computational Earth System Science, University of California: Santa Barbara, CA, USA.

[36] Liu, H., K. C. Jezek, B. Li, and Z. Zhao. 2015. Radarsat Antarctic Mapping Project Digital Elevation Model, Version 2. Boulder, Colorado USA. NASA National Snow and Ice Data Center Distributed Active Archive Center. doi: https://doi.org/10.5067/8JKNEW6BFRVD. [[Accessed 06 October 2020].

[37] Kalogirou, S. A. (2013). Solar energy engineering: processes and systems. Academic Press.

[38] Kreith, F., & Kreider, J. F. (1978). Principles of solar engineering. Washington.

[39] Sarbu, I., & Sebarchievici, C. (2016). Solar heating and cooling systems: Fundamentals, experiments and applications. Academic Press.

[40] Frey, R. A., Ackerman, S. A., Liu, Y., Strabala, K. I., Zhang, H., Key, J. R., & Wang, X. (2008). Cloud detection with MODIS. Part I: Improvements in the MODIS cloud mask for collection 5. Journal of Atmospheric and Oceanic Technology, 25(7), 1057-1072.

[41] Hocking, R. R., & Leslie, R. N. (1967). Selection of the best subset in regression analysis. Technometrics, 9(4), 531-540.

[42] James, G., Witten, D., Hastie, T., & Tibshirani, R. (2013). An introduction to statistical learning (Vol. 112, p. 18). New York: springer.

[43] Zhang, L., Gove, J. H., & Heath, L. S. (2005). Spatial residual analysis of six modeling techniques. Ecological Modelling, 186(2), 154-177.

[44] Wood, S. N., Pya, N., & Säfken, B. (2016). Smoothing parameter and model selection for general smooth models. Journal of the American Statistical Association, 111(516), 1548-1563.

[45] Wood, S. N. (2006). Low-rank scale-invariant tensor product smooths for generalized additive mixed models. Biometrics, 62(4), 1025-1036.

[46] Wood, S. N. (2017). Generalized additive models: an introduction with R. CRC press.

[47] Hui, F., Kang, J., Liu, Y., Cheng, X., Gong, P., Wang, F., ... & Guo, Z. (2017). AntarcticaLC2000: The new Antarctic land cover database for the year 2000. Science China Earth Sciences, 60(4), 686-696.

Appendix

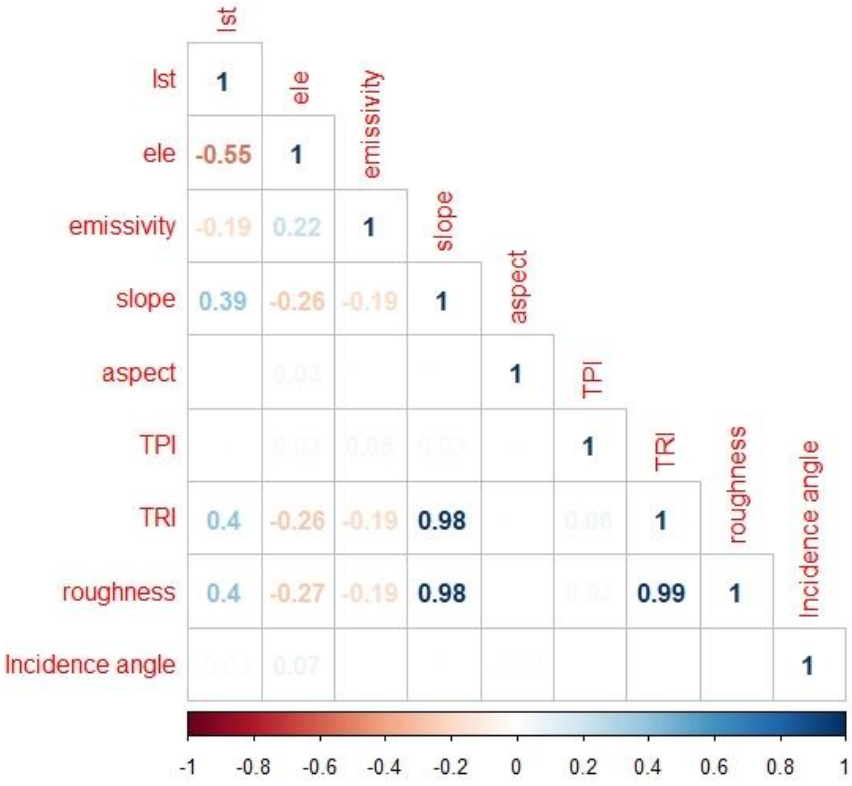

Figure 18. Correlation matrix between LST and predictors.